XVI IMEKO World Congress
Measurement - Supports Science - Improves Technology - Protects Environment ... and Provides Employment - Now and in the Future
Vienna, AUSTRIA, 2000, September 25-28

ACOUSTIC GAS TEMPERATURE AND FLOW MEASUREMENT

Y. Fukayama**, N. Morimoto**, H. Okimura**, H. Kitayama*
Babcock-Hitachi Kure Division* and Kure Research Laboratory**
3-36 Takara-machi, Kure 737-8508, Japan

Abstract: For acoustic measuring of gas temperature and flow, firstly, a processing method for microphone received signal based on the matched filtering with the pre-whitening to the AR modeled noises achieves good performance, in order to identify the time-of-flight under noise contamination. Then, the PRK (phase reversal keying) of the M-sequence appears to be proper for the testing signals, which are sent into the object. Finally, this system is validated through experiments.
Keywords: time-of-flight, matched filtering, M-sequence PRK

1 INTRODUCTION

Acoustic gas temperature and flow measurement system, which refers upstream and downstream time-of-flights of known wave of testing signals on acoustic paths in objects (ducts, furnaces etc.), is featuring non-contact and maintenance-free observation. For keeping accuracy on the measurement in applying audio frequency, which requires more economical sensors, and is more suitable for long distance or dusty acoustic paths than in ultrasonic frequency, not only the processing method for microphone received but also the testing signal wave sent into the objects have been optimized through this research.

Figure 1 shows the construction of acoustic gas temperature and flow measurement system. Flowing velocity V_f and sound speed V_s can be calculated from downstream and upstream time-of-flight in known distance L and angle θ as follows:

$$V_f = \frac{L}{2\cos\theta}\left(\frac{1}{t_{AB}} - \frac{1}{t_{BA}}\right),\quad V_S = \frac{L}{2\cos\theta}\left(\frac{1}{t_{AB}} + \frac{1}{t_{BA}}\right) \tag{1}$$

Then, gas temperature T_g is obtainable through the flowing.

$$T_g = \left(\frac{V_S}{\alpha}\right)^2 - 273.15 \tag{2}$$

where constant α depending on gas; conversion to mass flow from V_f and T_g as well.

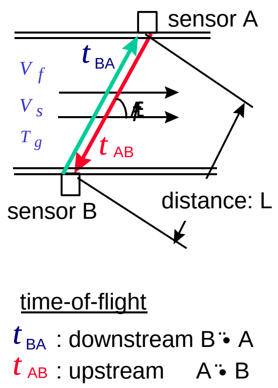

Fig.1 Temperature and flow measurement

2. SIGNAL PROCESSING METHOD

Through this research, the optimal condition of identifying the time-of-flight is regarded as the S/N maximum to the known testing wave before the threshold detector. Thus, following Thomas[4], the derivation for the seeking filter equation of the S/N maximum, which is under a given testing signal $\{s_k\}$ $(k = 0,1,\cdots,q)$ and an auto-correlation $r_N(n)$ of a noise sequence $\{N_m\}$, is applied.

Thus, assuming that the signal, which is contaminated with the noise, reached the microphone at 0 for simplicity, the filter output of the signal s_{oq} and the noise N_{oq} are respectively described in terms of a filter impulse response $\{h_k\}$ ($k = 0,1,\cdots,q$); thus, the signal-to-noise ratio at the destination $(\mathrm{S/N})_\mathrm{D}$ (after the processor) in energy at q is as follows:

$$(\mathrm{S/N})_\mathrm{D} = \frac{s_{oq}^2}{\mathrm{E}\{N_{oq}^2\}} = \frac{\left(\sum_{k=0}^{q} s_k h_{q-k}\right)^2}{\sum_{k=-\infty}^{q}\sum_{j=-\infty}^{q} r_N(k-j)h_{q-j}h_{q-k}} \quad \text{with} \quad s_{oq} = \sum_{k=-\infty}^{q} h_{q-k}s_k = \sum_{k=0}^{q} h_{q-k}s_k, \quad N_{oq} = \sum_{k=-\infty}^{q} h_{q-k}N_k \qquad (3)$$

where $s_k = 0 \;\; (k \le -1, q+1 \le k)$ are supplemented to the testing signal $\{s_k\}$.

Applying the variation technique, the seeking filter equation with the maximum condition of $(\mathrm{S/N})_\mathrm{D}$ in Eq.(3) is known to be as follows[1,4]:

$$\sum_{m=0}^{\infty} r_N(n-m)h_m^o = s_{q-n} \quad (n = 0,1,\cdots) \qquad (4)$$

where $\{h_n^o\}$ denotes the impulse response of the seeking optimal filter.

Finally, the seeking impulse response of the physically realizable (IUC) optimal filter has been obtained through the spectral factorization technique[1,4].

$$H^o(z) = \frac{1}{f_N^+(z)}\left[\frac{S(z^{-1})z^{-q}}{f_N^-(z)}\right]_+ = P(z)\left[P(z^{-1})S(z^{-1})z^{-q}\right]_+ \quad \text{with} \quad P(z) = \frac{1}{f_N^+(z)} \qquad (5)$$

where $H^o(z)$, $S(z)$ and $f_N(z)$ are bilateral Z-transform of $\{h_n^o\}$, $\{s_n\}$ and $r_N(n)$ in order; furthermore, $f_N^+(z)$, $f_N^-(z)$ respectively denote the IUC, OUC factors of power spectrum $f_N(z)$ of $\{N_m\}$.

Thus the seeking filter consists of a tandem connection of a pre-whitening filter of $P(z)$ and a succeeding filter which impulse response is the reverse order sequence of the q-step shifted output of the known testing signal $\{s_k\}$ after passing the whitening filter of $P(z)$.

Therefore, the seeking signal processor for the time-of-flight identification is shown in Fig.2. Before every testing signal sending, received noises have been identified as the AR coefficient a which will be applied for pre-whitening FIR filter. After signal sending, the matched filter refers the cross-correlation between pre-whitened microphone received v and known testing signal b in order to detect the peak of x.

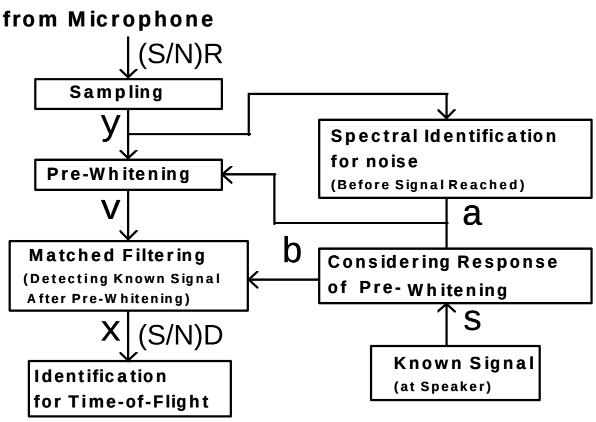

Fig.2 Processing flow for received signal

3. CHOICE OF TESTING SIGNAL

3.1 Matrices Expression of S/N

Since the optimal filter with the maximum S/N under a given testing signal $\{s_k\}$ and noise auto-correlation $r_N(n)$ has derived in the previous sections, then, how to give the optimal testing signal sent into the furnace and further maximizing the $(\mathrm{S/N})_\mathrm{D}$ the foregoing optimal filter shall be discussed in this section. At the beginning, in order to expect the $(\mathrm{S/N})_\mathrm{D}$, assuming that the signal reached the microphone at 0, the output x_q of the filter implemented in section 2 is expressed in the following matrices form.

$$x_q = s_{oq} + N_{oq} = \mathbf{s}^T \mathbf{U}^T \mathbf{U}(\mathbf{s}+\mathbf{N}_q), \text{ with } \mathbf{U} = \begin{pmatrix} 1 & -a_1 & \cdots & -a_p & 0 & 0 & \cdots & 0 \\ 0 & 1 & -a_1 & \cdots & -a_p & 0 & \cdots & 0 \\ 0 & 0 & 1 & -a_1 & \cdots & -a_p & \cdots & 0 \\ \cdots & \cdots & \cdots & \cdots & \cdots & \cdots & \cdots & \cdots \\ 0 & 0 & 0 & 0 & 0 & 0 & \cdots & 1 \end{pmatrix} \quad (6)$$

where $\mathbf{U}$ is $(q+1)\times(q+1)$ upper triangle matrix including the p-th order AR coefficients with assuming $p << q$. Furthermore, $\mathbf{N}_q$ is the random variable vector of the contaminating noise $\{N_m\}$, which auto-correlation matrix R_N is the $(q+1)\times(q+1)$ Toeplitz form not depending on subscript m under w.s.s. assumption.

In addition, the following relation is available.

$$\mathrm{U}\,\mathbf{N}_m = \mathbf{W}_m \text{ with } \mathbf{W}_m = \begin{pmatrix} W_m & W_{m-1} & \cdots & W_{m-q} \end{pmatrix}^T, \ \mathrm{E}\{W_m W_n\} = d_{m,n} r_W \quad (7)$$

where the first equation of Eqs.(7) suffices approximately in lower $p\ (p << q)$ lines, and $\mathbf{W}_m$ denotes the partial sequence vector of the white noise $\{W_m\}$.

At the next step, transposing the first equation of Eqs.(7) and taking expectation of both hands of it, then, multiplying U^{-1} and $(\mathrm{U}^T)^{-1}$ from left and right sides, the following is obtained.

$$\mathrm{R}_N^{-1} = \frac{1}{r_W} \mathrm{U}^T \mathrm{U} \quad (8)$$

Then, knowing the first equation of Eqs.(6), the S/N at q in matrices expression has been obtained.

$$(\mathrm{S/N})_{\mathrm{D}} = \frac{s_{0q}^2}{\mathrm{E}\{N_{0q}^2\}} = \frac{\left(\mathbf{s}^T \mathrm{R}_N^{-1} \mathbf{s}\right)^2}{\mathrm{E}\{\mathbf{s}^T \mathrm{R}_N^{-1} \mathbf{N}_q \mathbf{N}_q^T \mathrm{R}_N^{-1} \mathbf{s}\}} = \mathbf{s}^T \mathrm{R}_N^{-1} \mathbf{s} \quad (9)$$

3.2 Testing Signal for S/N Maximizing

In this section the optimal testing signal which maximize the foregoing filter is discussed based on the matrices S/N expression in Eq.(9) on condition of that the testing signal power is fixed.

Firstly, R_N in the Toeplitz form, which is a positive definite and symmetric matrix, has positive eigenvalues $\{l_0,\cdots,l_n,\cdots,l_q\}$ and the corresponding eigenvectors $\{\mathbf{e}_0,\cdots,\mathbf{e}_n,\cdots,\mathbf{e}_q\}$ which constitute an orthonormal set; therefore, any arbitrary testing signal can be expressed as the following form.

$$\mathbf{s} = \sum_{k=0}^{q} c_k \mathbf{e}_k \text{ with } \sum_{k=0}^{q} c_k^2 = 1 \quad (10)$$

where $c_k\ (k = 0,\cdots,q)$ are the expanding coefficients which are constrained on the unit signal power.

Then, knowing R_N^{-1} has the same orthonormal set of eigenvectors $\{\mathbf{e}_0,\cdots,\mathbf{e}_n,\cdots,\mathbf{e}_q\}$ with their eigenvalues $\{1/l_0,\cdots,1/l_n,\cdots,1/l_q\}$ and substituting Eq.(10) into Eq.(9) the S/N becomes and is bounded as follows:

$$\frac{1}{l_{\max}} = \frac{1}{l_{\max}} \sum_{k=0}^{q} c_k^2 \le \mathbf{s}^T \mathrm{R}_N^{-1} \mathbf{s} \le \frac{1}{l_{\min}} \sum_{k=0}^{q} c_k^2 = \frac{1}{l_{\min}} \quad (11)$$

where $l_{\max}$, $l_{\min}$, $\mathbf{e}_{\max}$, $\mathbf{e}_{\min}$ are the notations for the maximum and the minimum eigenvalues of R_N and their corresponding eigenvectors respectively.

While, knowing the Fourier series representation and referring Grenander et al.[2], R_N shall be expanded with the non-negative coefficients $\{g_0,\cdots,g_q\}$ as follows:

$$\mathrm{R}_N = g_0 \mathrm{I}_{q+1} + \sum_{k=1}^{q} g_k \mathbf{f}_k \mathbf{f}_k^* \quad \text{with} \quad \mathbf{f}_k = \begin{pmatrix} 1 & \exp(\mathrm{j}w_k) & \cdots & \exp(\mathrm{j}qw_k) \end{pmatrix}^T \tag{12}$$

where g_0, the superscript * and $\mathbf{f}_k$ respectively denotes the white noise component, the transpose of the complex conjugate, and sinusoidal vectors with the angular frequency w_k.

Thus, considering the eigenvalues l_k and the eigenvectors $\mathbf{e}_k$ of R_N, the following relation has to be sufficed.

$$\left(g_0 \mathrm{I}_{q+1} + \sum_{k=1}^{q} g_k \mathbf{f}_k \mathbf{f}_k^* \right) \mathbf{e}_n = l_n \mathbf{e}_n \quad (n = 0,\cdots q) \tag{13}$$

As knowing the $\mathrm{span}\{\mathbf{f}_1,\cdots \mathbf{f}_q\}$ is the dimension of not more than q and is a sub-space of the $\mathrm{span}\{\mathbf{e}_0,\cdots,\mathbf{e}_n,\cdots,\mathbf{e}_q\}$ which dimension is $q+1$, there exists at least an eigenvector $\mathbf{e}^o$ which is orthogonal to the $\mathrm{span}\{\mathbf{f}_1,\cdots \mathbf{f}_q\}$; then, Eq.(13) becomes as follows:

$$g_0 \mathrm{I}_{q+1} \mathbf{e}^o = l^o \mathbf{e}^o \tag{14}$$

where l^o is the corresponding eigenvalue to $\mathbf{e}^o$

Consequently, comparing Eq.(13) with Eq.(14), any eigenvalue $l_n \; (\neq l^o)$ corresponding to $\mathbf{e}_n$, which is not orthogonal to the $\mathrm{span}\{\mathbf{f}_1,\cdots \mathbf{f}_q\}$, is greater than l^o according to the non-negative of $\{g_0,\cdots,g_q\}$; therefore, the following properties of the optimal testing signal have been obtained with referring Willet et al.[5].

$$l_{\min} = l^o = t_0, \; \mathbf{s} = \mathbf{e}_{\min} = \mathbf{e}^o \quad \text{with} \quad (\mathrm{S/N})_{\mathrm{Dmax}} = \frac{s_{oq}^2}{\mathrm{E}\{N_{oq}^2\}} = \frac{1}{g_0} \;\; \left(\text{under } \sum_{k=0}^{q} c_k^2 = 1\right) \tag{15}$$

where, knowing Eq.(15), the upper bound of $(\mathrm{S/N})_{\mathrm{D}}$ above has also been obtained.

3.3 Implementation of Optimal Signal

According to the result of section 3.2, the M-sequence $\{w_k\}$, which auto-correlation is nearly equal to that of the white noise and generated through the following manner, shall be considered as the testing signal. In this implementation, the binary sequence $\{w_k\}$ is sent into boiler furnaces by way of the PRK (Phase Reversal Keying) shown in Fig.3.

$$s_n = \mathrm{s}((\mathrm{n}-1)\Delta \mathrm{t}) \quad \text{with} \quad \mathrm{s}(t) = (2w_k - 1)\sin(2pft), \quad w_k = w_{k-r} \oplus w_{k-r+m} \quad (\mathrm{m} = 1,\cdots,\mathrm{r}-1) \tag{16}$$

where an r-th order shift register with a proper initial value $(0 \text{ or } 1)$ is prepared, and the operation $\oplus$ denotes the exclusive-or. In addition, $\mathrm{s}(t)$ and f are respectively the speaker driving signal and the carrier frequency. In this connection, the foregoing sequence $\{s_n\}$ is obtained through sampling on $\Delta\mathrm{t}$ period.

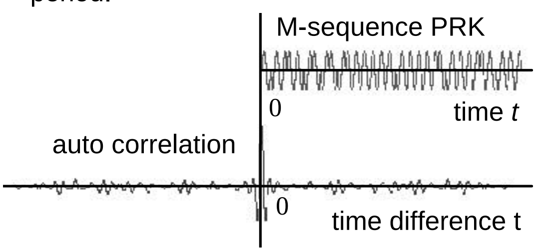

Fig.3 Testing Signal for Acoustic Measurement

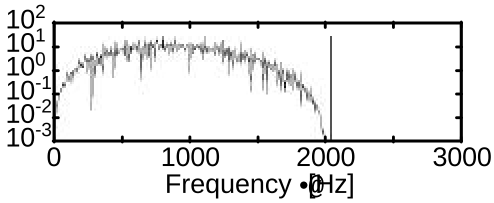

Fig.4 FFT example of M-sequence PRK

By the way, the spectrum of $\mathrm{s}(t)$ is just the same as that of the DSB-SC (Double Side Band with

Suppressed Carrier) modulation for the M-sequence which forms lower and upper side bands of spectrum $\left(\frac{f}{2^r-1}, f\right)$ around the suppressed line spectrum of the carrier at f ; namely, wide spectrum in $(0, 2f)$ shown in Fig.4, like the white noises, which are required through the discussions in section 3.2.

4. VALIDATION

4.1 Processed Signal in a Commercial Plant

Acoustic measurement in this paper has been applied to a boiler at a 1000MWe power plant where sensors are equipped on the furnace wall shown in Fig.5. Figure 6 is an example of processed signal under considerably strong colored noise (S/N before the processor: $(\mathrm{S/N})_{\mathrm{R}} = 0.14$) in the furnace. Though such a severe condition, processed signal x with the processor in Fig.2 provides a clear peak for the time-of-flight identification.

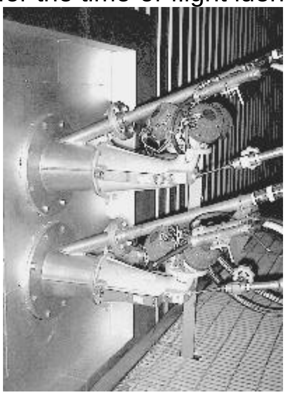

Fig.5 Sensors on furnace wall

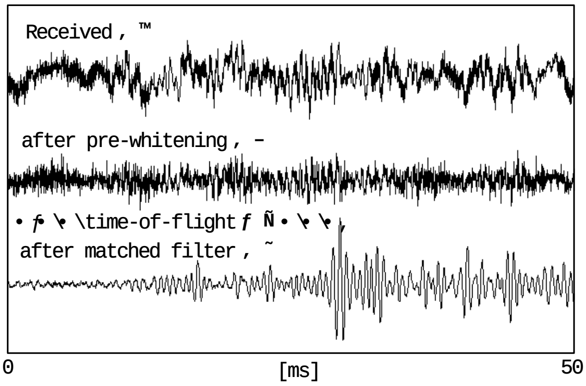

(signal: M-sequence PRK, processor: Fig.2)
Fig.6 Identified time-of-flight

4.2 Temperature Measurement

The gas temperature measurement was firstly validated on an experimental furnace shown in Fig.7 at a laboratory. Figure 8 indicates that the standard deviation of difference between acoustic measured and reference, spatial average based on the five-point thermocouple measurement, is about three degree, which should be considered as exellent value.

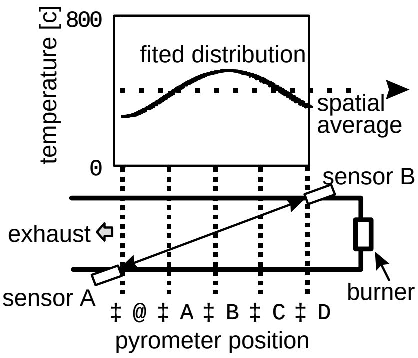

Fig.7 Gas temperature validation

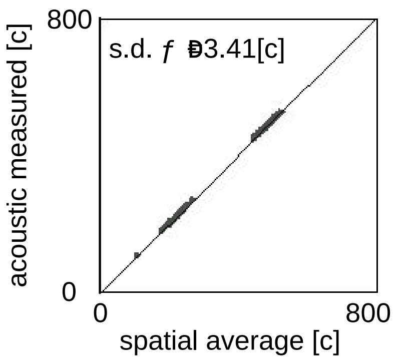

Fig.8 Validated temperature at a laboratory.

Then the validation took place at a 1000MW thermal power station with sensors in Fig.5, which measuring distance between the speaker and the microphone is over 30m. Figure 9 shows an example of the measurement during a load rejection (emergency shut-down) test and re-start-up operation. Though such fast changing, the measurement system can clearly grasp the transient gas temperature after the test. Furthermore, the sufficient accuracy of the temperature measurement is validated in Fig.10 through comparison with reference by temporary-set-up suction pyrometer, which consists a thermocouple in a sheath and a gas ejector for avoiding error from radiation.

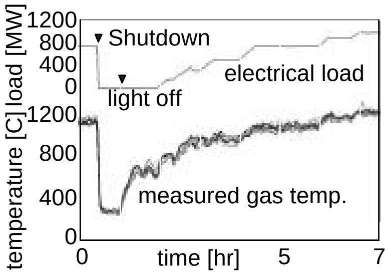

Fig. 9 Measurement at a 1000MWe boiler

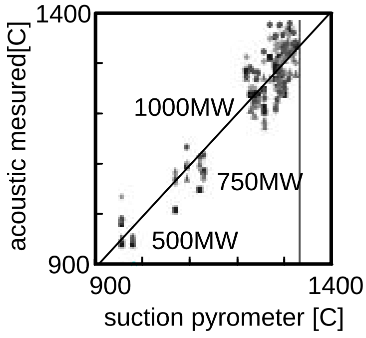

Fig.10 Validated temperature at the boiler

4.3 Flow Measurement

Figure 11 shows an example of flow measurement swinging up to 30 m/s velocity condition at a field duct. The sufficient accuracy through validation tests referring a linear resistance type flow meter in low velocity region and difference pressure type in high region are indicated in Fig.12.

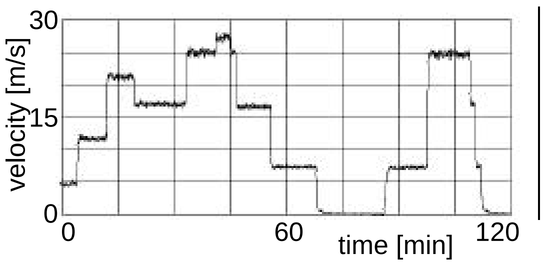

Fig.11 Measurement at a field duct

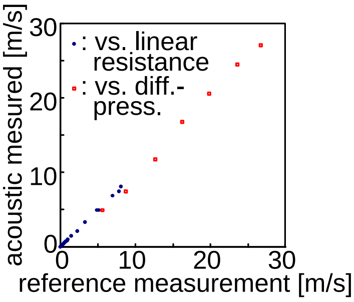

Fig.12 Validated flow at the duct

Through above mentioned validation of temperature and flow, the adequacy of the technique in this report has been cleared.

5. CONCLUSIONS

Acoustic gas temperature and flow measurement with the following features has been developed:

1. A signal processing method based on the Matched filter and the Pre-whitener which are successively renewed through an on-line spectral identification of noises in the boiler furnaces.
2. A testing signal of the phase reverse keying of the M-sequence with sharp auto-correlation suitable for identifying time-of-flight.
3. Validated temperature and flow measurement accuracy through laboratory and field testing.
4. Applied on a boiler of a commercial power plant which measuring distance is over 30m.

REFERENCES

[1] Fukayama, Y et al.: Acoustic Gas Temperature Measurement for Controlling Boilers; Proceeding of Japan/USA. Symposium on Flexible Automation, pp.433-440, ASME 1996

[2] Grenander, U. and Szego, G.: Toeplitz Forms and Their Applications; Univ. of California, 1958.

[3] Imada, N. et al.: Measurement of Gas Temperature Distribution in Recovery Boilers Using Acoustic CT Method; Proc. of JSME-ASME Intl. Conf. on Power Engineering, Vol.1, pp.227-230, 1993

[4] Thomas, J. B.: An Introduction to Communication Theory and Systems; Springer, New York, 1988

[5] Willet, P. K., and Thomas, J. B.: Signal Choice for the Finite-Length Matched Filter; Proc. of 21st Conf. in Information Science and Systems, pp.94-99, USA